Aromatic Copolyesters with Stilbene Mesogenic Groups. 2. Synthesis and Thermal Behavior

Jean Pierre Leblanc,[†] Martine Tessier,[†] Didier Judas,[‡] Claude Friedrich,[§] Claudine Noël,*,[§] and Ernest Maréchal[†]

Laboratoire de Synthèse Macromoléculaire, CNRS, URA 24, Université P. et M. Curie, 4 Place Jussieu, 75252 Paris Cedex 05, France, ELF ATOCHEM, CERDATO, 27470 Serquigny, France, and Laboratoire de Physicochimie Structurale et Macromoléculaire, CNRS, URA 278, ESPCI, 10 Rue Vauquelin, 75231 Paris Cedex 05, France

ABSTRACT: A number of wholly aromatic copolyesters were prepared from methylhydroquinone diacetate, stilbenedicarboxylic acid, and at least one of the following diacids: isophthalic acid, terephthalic acid, and 4,4'-oxydibenzoic acid. The copolyesters were characterized by DSC, optical microscopy, and X-ray diffraction. The effects of composition on the thermal and structural characteristics of the materials were evaluated. Annealing after-treatments were also carried out. The results of different thermal treatments showed that copolyesters were substantially affected by thermal treatments in terms of both transition temperatures and structures.

Introduction

Aromatic copolyesters undoubtedly represent the most important class of thermotropic nematics. Our specific interest in aromatic copolyesters containing stilbene units originated from the finding that, in accordance with the general requirement of an elongated and fairly rigid molecular structure, derivatives of stilbene provide liquid crystals of high thermal stability. In the first paper of this series, the effects of the molecular structure and geometry (anisotropy, rigidity, linearity, planarity, ...) of aromatic moieties and of the specific details of linking groups on the liquid crystal properties of some low molar mass compounds were illustrated by reference to compounds containing a terephthaloyl, a hydroquinone, or a stilbene central unit in the mesogenic core.[1]

In this investigation, a number of wholly aromatic copolyesters have been prepared by copolycondensation of methylhydroquinone diacetate (MH) with stilbene-dicarboxylic acid (S) and at least one of the following diacids: isophthalic acid (I), terephthalic acid (T), and 4,4'-oxydibenzoic acid (ODB). MH, I, and ODB were employed for reducing the melting temperature by disrupting the perfect regularity of simple but intractable para-linked aromatic polymers.[2] Indeed, lateral substitution of the aromatic ring (e.g. MH) decreases molecular symmetry. Introduction of kinks or bends based on essentially rigid units (e.g. I) depresses the diffusion of the crystalline solid by reducing the probability of finding a run of crystallizable units. Use of flexible bonds such as −O− (e.g. ODB) tends to increase the entropy of the melt. In general, these alterations also tend to decrease the axial ratio of the molecule. As a result, the thermal stability range of the mesophase is reduced and the liquid crystalline behavior may eventually disappear.

Annealing after-treatments of the "as-made" copolyesters were also carried out and the thermal and structural characteristics of the materials determined. The effects of annealing on the structure of wholly aromatic liquid crystalline copolyesters have been studied extensively.[3–14] Annealing resulted in an increase in the melting temperature and enthalpy change. A significant increase in the three-dimensional order was also evident. Usual estimates of percent crystallinity range from 10–20% for "as-made" or slowly cooled samples[7,8,12,15] to as high as 65% in heat-treated samples.[4–8] The surprising finding was, however, that the values observed for the entropy and enthalpy of fusion, normalized to the fraction of the ordered state present, were much lower[3,4,6–9,15] than the ones usually encountered in conventional polymers (ΔH_0 = 20–50 kJ/mol and ΔS_0 = 40–100 J/(mol·K)[16,17]). The low enthalpy of fusion was rationalized in terms of disorder in the crystalline species,[7,8,11,15] as was evident from the limited diffraction effects, while the low entropy of fusion was explained on the basis that there is little change in the configurational entropy when rigid chains in a crystal are taken to the rigid chain melt state.[9,15] It should be noted that the aromatic moieties in most of the copolyesters studied so far have outgoing bonds that are either colinear (*p*-phenylene) or parallel (2,6-naphthylene). In contrast, the copolyesters studied here contain angular entities (*m*-phenylene and/or ether oxygen) which may substantially affect crystallization behavior. Recently, Erdemir et al.[18] and Blundell et al.[19] have shown that two of the crystal forms observed in poly(*p*-oxybenzoate-*co*-*p*-phenylene isophthalate)s contain the kinked *m*-phenylene units. One is associated with cooling from the nematic phase and exhibits a relatively high enthalpy of fusion compared to the values obtained for thermotropic copolyesters containing rigid, straight base units.

Experimental Part

Materials. Monomers and Model Compounds. Isophthalic and terephthalic acids (both laboratory reagents from Aldrich Chemical Co.) were used as received without any further purification. Stilbenedicarboxylic acid was prepared and purified according to the procedures developed by Toland.[20] 4,4'-Oxydibenzoic acid was prepared by the process first described by McIntyre.[21]
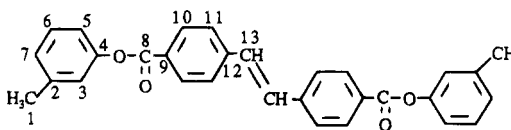
Methylhydroquinone Diacetate. It was prepared by treating methylhydroquinone (1.0 mol, 124.14 g) and acetic anhydride (2.1 mol, 214.2 g) in the presence of a catalytic amount of H_2-
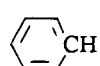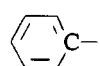

[†] Laboratoire de Synthèse Macromoléculaire.
[‡] ELF ATOCHEM.
[§] Laboratoire de Physicochimie Structurale et Macromoléculaire.

**Table 1. ^{13}C NMR Spectrum of 3,3′-Ditolyl
trans-4,4′-Stilbenedicarboxylate in DMSO-d_6 Solution**

group	δ (ppm)	assignment
-CH₃	20.66	C^1
-CH=	129.45	C^{13}
⟨CH⟩	118.70	C^5
	122.16	C^3
	126.93	C^7, C^{11}
	128.57	C^{10}
	129.08	C^6
⟨C−⟩	126.43	C^9
	139.16	C^2
	146.34	C^{12}
	150.55	C^4
⟩C=O	164.30	C^8

**Table 2. ^{13}C NMR Spectrum of 3,3′-Ditolyl
4,4′-Oxydibenzoate in DMSO-d_6 Solution**

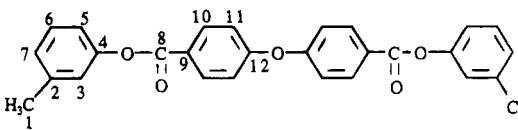| group	δ (ppm)	assignment
-CH₃	20.71	C^1
⟨CH⟩	118.73	C^5
	119.09	C^{11}
	122.17	C^3
	126.54	C^7
	129.17	C^6
	132.34	C^{10}
⟨C−⟩	124.72	C^9
	139.24	C^2
	150.58	C^4
	160.13	C^{12}
⟩C=O	163.83	C^8

SO₄(c) (4 drops). The reaction was allowed to proceed for 2 h before the reaction mixture was poured into water. The crude product was crystallized from a 1/1 ethanol–water mixture. Mp: 43 °C. Yield: 70%.

3,3′-Ditolyl trans-4,4′-Stilbenedicarboxylate. A mixture of thionyl chloride (0.01 mol, 1.2 g), pyridine (10 mL), and methylene chloride (10 mL) was kept at 0 °C for 10 min. S (0.003 mol, 0.8 g) in pyridine (20 mL) was added dropwise (addition time: 20 min), and the reaction mixture was stirred at room temperature for 30 min. m-Cresol (0.0084 mol, 0.9 g) in pyridine (10 mL) was then added, and the reaction was carried out at 80 °C for 5 h. The reaction mixture was poured into a 1/1 ethanol–water mixture, and the product was washed three times with boiling ethanol. Mp: 245 °C. Yield: 67%. The ^{13}C NMR spectrum was consistent with the assigned structure (Table 1). Anal. Calcd for C₃₀H₂₄O₄: C, 80.34; H, 5.39; O, 14.27. Found: C, 80.12; H, 5.15; O, 14.48.

3,3′-Ditolyl 4,4′-Oxydibenzoate. To a mixture of benzenesulfonyl chloride (0.0065 mol, 1.15 g), LiCl (0.005 mol, 0.21 g), and pyridine (5 mL), was added a solution of ODB (0.0025 mol, 0.645 g) in pyridine (5 mL). The reaction mixture was maintained at room temperature for 10 min and then heated to 115 °C with vigorous stirring. A solution of m-cresol (0.005 mol, 0.54 g) in pyridine (10 mL) was added dropwise (addition time: 30 min), and the reaction mixture was maintained at 115 °C for 3 h. After cooling, the mixture was poured into a 1/1 ethanol–water mixture (300 mL) and the product crystallized from the same mixture. Mp: 101 °C. Yield: 76%. The ^{13}C NMR spectrum was consistent with the assigned structure (Table 2). Anal. Calcd for C₂₈H₂₂O₅: C, 76.70; H, 5.06; O, 18.24. Found: C, 76.72; H, 4.85; O, 18.04.

3,3′-Ditolyl Terephthalate. It was prepared in a similar manner. Mp: 170 °C. Yield: 83%. The ^{13}C NMR spectrum was consistent with the expected structure (Table 3). Anal. Calcd for C₂₂H₁₈O₅: C, 76.29; H, 5.24; O, 18.47. Found: C, 76.39; H, 5.03; O, 18.45.

3,3′-Ditolyl Isophthalate. To a solution of isophthaloyl chloride (0.015 mol, 3.04 g) in pyridine (25 mL) was added a solution of m-cresol (0.038 mol, 4.10 g) in pyridine (25 mL). The reaction was allowed to proceed at room temperature for 24 h with vigorous stirring before the reaction mixture was poured into water. The crude product was washed with warm water and crystallized from a 1/1 ethanol–water mixture. Mp: 102.3 °C. Yield: 85%. The ^{13}C NMR spectrum was consistent with the assigned structure (Table 4). Anal. Calcd for C₂₂H₁₈O₅: C, 76.29; H, 5.24; O, 18.47. Found: C, 75.68; H, 5.05; O, 18.32.
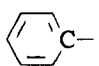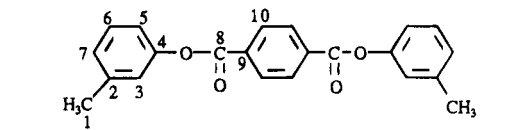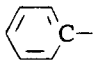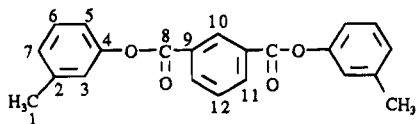
**Table 3. ^{13}C NMR Spectrum of 3,3′-Ditolyl Terephthalate
in CDCl₃ Solution**

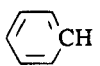| group	δ (ppm)	assignment
-CH₃	21.28	C^1
⟨CH⟩	118.49	C^5
	127.12	C^7
	129.37	C^6
	122.13	C^3
	130.33	C^{10}
⟨C−⟩	134.01	C^9
	139.93	C^2
	150.68	C^4
⟩C=O	164.84	C^8

The principal features of the X-ray powder patterns for 3,3′-ditolyl *trans*-4,4′-stilbenedicarboxylate (3TS), 3,3′-ditolyl 4,4′-oxydibenzoate (3TODB), 3,3′-ditolyl terephthalate (3TT), and 3,3′-ditolyl isophthalate (3TI) are given in Table 5. Molecules are aligned with their long axes approximately in the crystallographic *C* direction. For 3TT a lamellar thickness of about 15 Å is obtained in good agreement with the molecular length estimated for the most extended conformation (L = 15.6 Å). Preliminary consideration of the d spacings suggests an orthorhombic unit cell with a = 6.05, b = 7.53, and c = 15.07 Å. The molecules of 3TI and 3TODB pack with significant overlap occurring between the terminal rings of adjacently stacked molecules. This result is in agreement with recent diffraction studies of diphenyl isophthalate[22] which suggest an orthorhombic lattice with a = 6.46, b = 7.66, and c = 32.87 Å.

Polyesters and Copolyesters. Polyesters and copolyesters were prepared in the melt by polycondensation of the appropriate monomers in the absence of catalyst. The polycondensation was conducted in two stages. In the first stage,

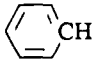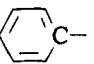**Table 4. ^{13}C NMR Spectrum of 3,3′-Ditolyl Isophthalate in CDCl$_3$ Solution**

group	δ (ppm)	assignment
-CH$_3$	21.30	C^1
	118.57	C^5
	126.90	C^7
	129.27	C^6
	129.04	C^{12}
	122.20	C^3
	131.70	C^{10}
	134.83	C^{11}
	130.57	C^9
	130.78	C^2
	150.87	C^4
>C=O	164.31	C^8

Table 5. Principal Reflections (Å) of Model Compounds 3,3′-Ditolyl 4,4′-Stilbenedicarboxylate (3TS), 3,3′-Ditolyl 4,4′-Oxydibenzoate (3TODB), 3,3′-Ditolyl Terephthalate (3TT), and 3,3′-Ditolyl Isophthalate (3TI)

3TS	3TODB	3TT	3TI
13.73^a (s)	21.98^a (s)	15.09^a (s)	17.13^a (s)
9.80 (s)	11.14^a (w)	7.52^a (m)	8.7^a (w)
6.89^a (s)	7.91 (w)	6.71 (m)	7.55 (m)
6.53 (w)	7.36^a (w)	5.99 (m)	6.06 (s)
5.76 (s)	6.70 (m)	5.63 (w)	5.0 (w)
5.36 (m)	5.76 (w)	5.26 (w)	4.7 (s)
4.82 (s)	5.56^a (w)	5.02^a (m)	4.29^a (m)
4.64 (m)	5.12 (vw)	4.75 (vw)	4.15 (m)
4.28 (s)	4.65 (vs)	4.48 (m)	4.04 (m)
3.79 (w)	4.38^a (s)	4.20 (w)	3.88 (m)
3.66 (s)	4.15 (w)	3.77^a (s)	3.76 (s)
3.49 (m)	4.00 (vs)	3.63 (m)	3.39 (s)
3.26 (w)	3.67^a (m)	3.52 (w)	3.29 (w)
3.13 (w)	3.55 (vw)	3.38 (w)	3.20 (m)
	3.38 (m)	3.19 (w)	3.02
	3.26 (s)		2.96
	3.12 (w)		

^{a} Diffraction peaks which are chain-length-dependent (001) type reflections. Relative intensity: vs, very strong; s, strong; m, medium; w, weak; vw, very weak.

the reaction was carried out under nitrogen flow, while in the second stage, the pressure was reduced to 0.1 Torr.

Monomers (MH excess: 5%) were charged into a cylindrical reactor fitted with a stirrer, a nitrogen inlet, and a downward directed condenser. The reactor was purged with dry nitrogen and placed in either a salt mixture (KNO$_3$ 57%, NaNO$_3$ 7%, NaNO$_2$ 40%) or a Wood alloy bath preheated at a temperature 20 deg below the polycondensation temperature. The reaction mixture was then rapidly heated to the polycondensation temperature and maintained at that temperature under nitrogen flow until most of the acetic acid was evolved.

During this first stage of the reaction, the condenser was connected to a capillary tube immersed in a solution of thymol blue in ethanol. The extent of the reaction was determined by titrating the acetic acid collected in the receiver by 1 N sodium hydroxide.

The next stage was carried out under vacuum. The capillary tube was replaced by a receiver, and the pressure was gradually decreased to 0.1 Torr while the temperature of the mixture was raised. The distillate was cooled by liquid nitrogen and titrated by 1 N sodium hydroxide.

Table 6. Polyesters Based on MH, I, S, T, or ODB

| polyester | polymerization conditions | | conversion (%) | |
	1st stage (N$_2$) T (°C), t (min)	2nd stage (0.1 Torr) T (°C), t (min)	a	b
MH/I	270, 120	310, 165	75	94
MH/S	270–320, 180	320–330, 180	35	75
MH/T	270–320, 160	320–330, 180	72	91
MH/ODB	270–310, 120	310–330, 180	78	96

The conditions selected for the preparation of the polyesters and copolyesters are listed in Tables 6–9 where a and b are the conversion at the end of the first stage of the reaction and the global conversion, respectively. In all cases, the molar ratio of MH to diacids was kept constant at 1.05.

Analytical Techniques. Inherent viscosities of copolyesters based on MH, I, S, and ODB were measured in *p*-chlorophenol at 0.1 g/dL concentration.

High-resolution ^{13}C NMR spectra were recorded on a 250 FT Brüker spectrometer using the XHCORR impulsion sequence ($\Delta_1 = 0.5J_{C-H}$ with $J_{C-H} = 140$ or 10 Hz) in the case of 2D-NMR ^{13}C–^{1}H spectra.

Solid state ^{13}C NMR spectra were recorded at 79.47 MHz on a Brüker CXP 300 spectrometer.

Thermal transition characteristics were established by using differential scanning calorimetry (DSC), with heating and cooling cycles carried out in a DuPont 910 differential scanning calorimeter. The sample size was typically 10 mg, with runs performed at a heating rate of 10 °C/min. T_g was estimated from the point of intersection between the initial baseline and the sloping portion of the line obtained as the baseline shifts during the glass transition. The maxima of the endotherms were taken as the melting and isotropization transition temperatures.

The assignment of the transitions was confirmed using a polarizing microscope (Olympus BHA-P or Leitz Larborlux 12 Pol.) equipped with a hot stage (Mettler FP5 or Linkam THM 600) and by observing the behavior of polymers protected by glass cover slips. To minimize in situ specimen polycondensation and/or degradation, the hot stage was preheated to the desired temperature, before the samples were mounted. Specimens that did not flow spontaneously when heated above their transition temperatures were subjected to shear by pressing on the upper cover slip with a dissecting needle. The complete disappearance of melt birefringence was taken as the clearing point.

Thermal stability was assessed by thermogravimetric analysis (DuPont 9900-TGA 951) carried out under nitrogen.

Wide angle X-ray diffraction patterns were recorded on flat films using Cu Kα radiation. A flat graphite crystal with a pinhole collimator was used as a monochromator. The samples were contained in 1 mm Lindemann glass tubes. Oriented polymeric samples were produced by drawing fibers out of the mesophase with a pair of tweezers.

Results and Discussion

Synthesis of Copolyesters. Copolyesters Based on MH, I, and S. Three of the present authors have previously shown that I dissolves and readily reacts with MH at and above 260 °C.[23] Before preparing the copolyesters, we have compared the reactivities of S and I by studying the model condensation reactions of these two diacids with β-naphthol acetate which does not lead to polycondensates and whose volatility is sufficiently low to avoid material losses at high temperatures. The reactions were followed by titrating collected acetic acid. The results are summarized in Figure 1. At 280 °C, the reactivity of S is much lower than that of I: there is no significant condensation of S with β-naphthol acetate before 50 min. This period corresponds to the time required for the formation of a homogeneous mixture. However, at 310 °C the rates of the reactions of S and I with β-naphthol acetate are similar although

Table 7. Copolyesters Based on MH, I, and S

| | | polymerization conditions | | conversion (%) | |
| | composition | 1st stage (N_2) | 2nd stage (0.1 Torr) | | |
copolyester	I/S (mol %)	T (°C), t (min)	T (°C), t (min)	a	b
A1	85/15	290–310, 135	310, 120	84	92
A2	80/20	290, 135	305, 150	76	84
A3	80/20	290–320, 110	320, 120	86	97
A4	75/25	290–310, 105	310, 120	85	91
A5	70/30	260, 90 then 310, 60	310, 120	85	89
A6	65/35	260, 60 then 300, 60	305, 120	65	86
A7	65/35	260, 60 then 310, 180	320, 120	90	95
A8	50/50	290, 180	290, 150	26	47
A9	50/50	295, 180	300, 120	48	72.5
A10	50/50	270, 60 then 280, 90 then 305, 150	310, 120	72	94

Table 8. Copolyesters Based on MH, I, S, and ODB

| | | polymerization conditions | | conversion (%) | |
| | composition I/ODB/S (mol%) | 1st stage (N_2) | 2nd stage (0.1 Torr) | | |
copolyester		T (°C), t (min)	T (°C), t (min)	a	b
B1	50/50/0	270–290, 120	290–310, 160	76	97
B2	76/5/19	280–290, 240	290–310, 135	77	84
B3	72/10/18	285–300, 300	305–315, 150	78	90
B4	64/20/16	270–300, 240	310, 180	78	87
B5	60/20/20	265, 180 then 280, 120	320, 120 then 335, 10	74	87
B6	50/30/20	265, 300	320, 150 then 345, 10	74	86
B7	45/45/10	290, 300	320, 120	64	85
B8	33.3/33.3/33.3	260–305, 195	315, 150	74	82
B9	20/40/40	250–300, 210	300–340, 120	68	95

Table 9. Copolyesters Based on MH, S, ODB, and T

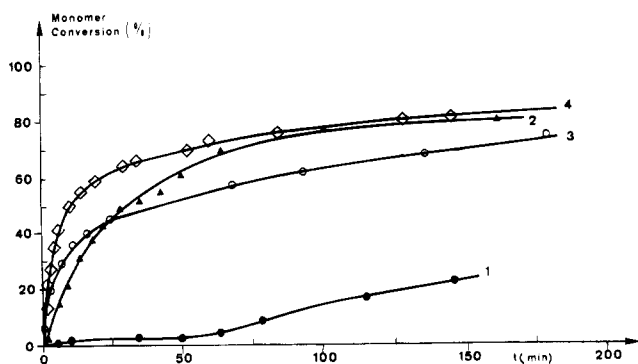| | | polymerization conditions | | conversion (%) | |
| | composition T/ODB/S (mol %) | 1st stage (N_2) | 2nd stage (0.1 Torr) | | |
copolyester		T (°C), t (min)	T (°C), t (min)	a	b
C1	50/50/0	265–280, 150	280–330, 150	84	98
C2	47.5/47.5/5	265, 180 then 270, 60	270–330, 150	75	90
C3	45/45/10	270, 120 then 270–300, 90	310–340, 135	75	85

Figure 1. Conversion (%) calculated from collected acetic acid versus time (min) in the reaction of I and S with β-naphthol acetate. $T = 280$ °C: I (○); S (●). $T = 310$ °C: I (◇); S (▲).

the reactivity of S is slightly lower for reaction times shorter than 80 min. Again, this can be ascribed to the nonhomogeneity of the S–β-naphthol acetate mixtures. It should be noted that the solubility of S in β-naphthol acetate is greatly improved in the presence of I. These results led us to select the following method for the preparation of copolyesters.

An excess (5%) of MH was incorporated to compensate for the losses due to the volatility of this compound under experimental conditions and to some side reactions such as the formation of methylhydroquinone or methylhydroquinone monoacetate.[23] The polycondensation was conducted in two stages. In the first stage, the reaction was carried out under nitrogen flow at 270–310 °C to favor S condensation while minimizing MH losses. In the second stage, the pressure was

gradually reduced to 0.1 Torr and the temperature was raised, unless otherwise stated, to 310–320 °C. It was noted that the reaction mixtures with I/S ≤ 80/20 mol % exhibited signs of stir opalescence typical of a nematic mesophase. Data for the preparation of copolyesters MH/I/S are collected in Table 7. Regardless of S content, the conversion was relatively high (86–97%). As expected, however, by using the same procedure but with a lower polymerization temperature in the second stage of the reaction, it was possible to decrease the conversion (see Table 7, A2, A6, A8, and A9).

Conventional high-resolution NMR cannot be utilized as a characterization technique for these copolyesters which are essentially insoluble unless subjected to extensive degradation so that the structure of copolyesters was verified by solid state ^{13}C NMR (Figure 2a). The chemical shifts compare nicely with those deduced from the liquid state ^{13}C NMR spectra of 3,3'-ditolyl stilbenedicarboxylate (Table 1) and 3,3'-ditolyl isophthalate (Table 4) and the solid state ^{13}C NMR spectra of homopolyesters based on MH and I (Figure 2b) or S (Figure 2c). They are in good agreement with data obtained for aromatic copolyesters containing isophthaloyl and/or methylhydroquinone units.[23-25]

Copolyesters Based on MH, I (or T), S, and ODB. These copolyesters were also prepared, without added catalyst, by melt polycondensation of the appropriate monomers. The polymerization procedure was similar to that described above. Tables 8 and 9 summarize polymerization conditions employed for the copolyesters of each series. The global conversions lie in the range 82–95%.
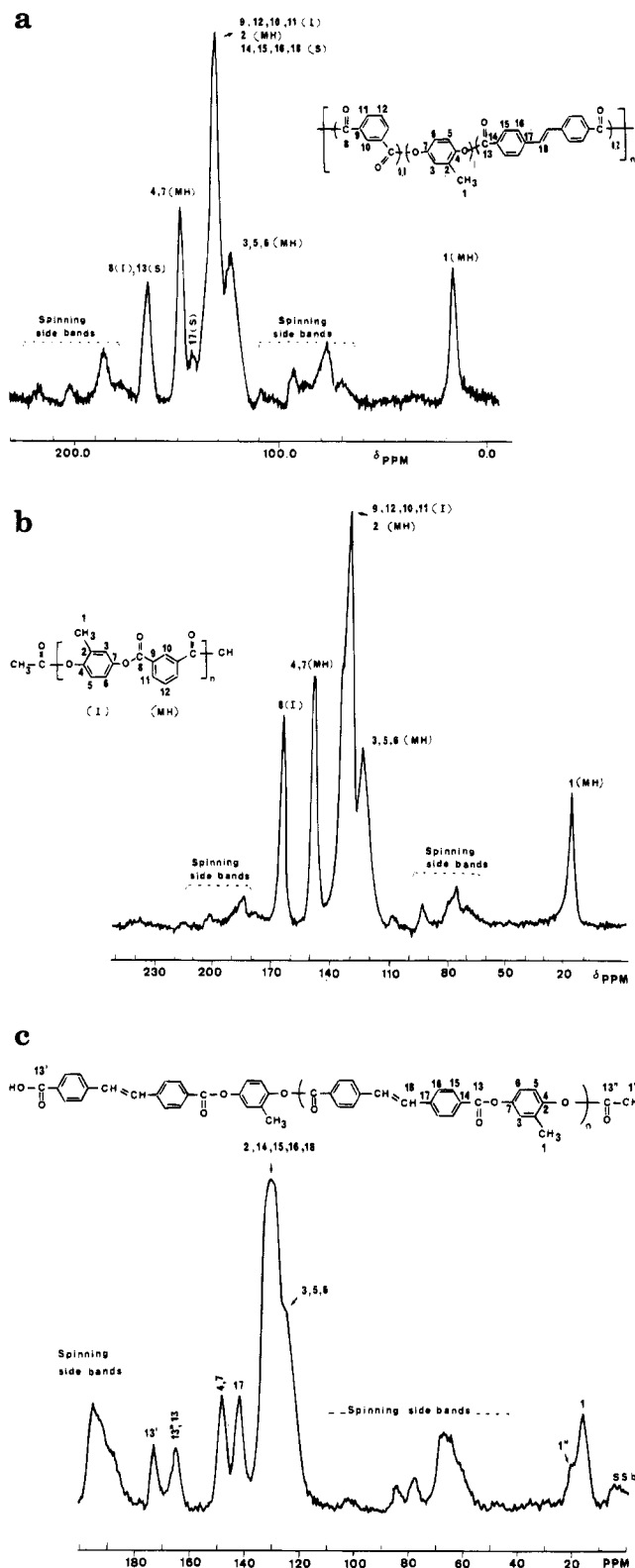
Figure 2. Solid state ^{13}C NMR spectra: (a) copolyester A2; (b) polyester MH/I; (c) polyester MH/S.

Figure 3. Solid state ^{13}C NMR spectra: (a) copolyester B8; (b) polyester MH/ODB.

The solid state ^{13}C NMR spectra were consistent with the expected structures. Representative spectra are shown in Figures 3 and 4. The chemical shifts compare well with those deduced from the liquid state ^{13}C NMR spectra of model compounds (Tables 1–4) and the solid state ^{13}C NMR spectra of homopolyesters based on MH and one of the diacids: I (Figure 2b), T (Figure 4b), S (Figure 2c), or ODB (Figure 3b). They are in good agreemen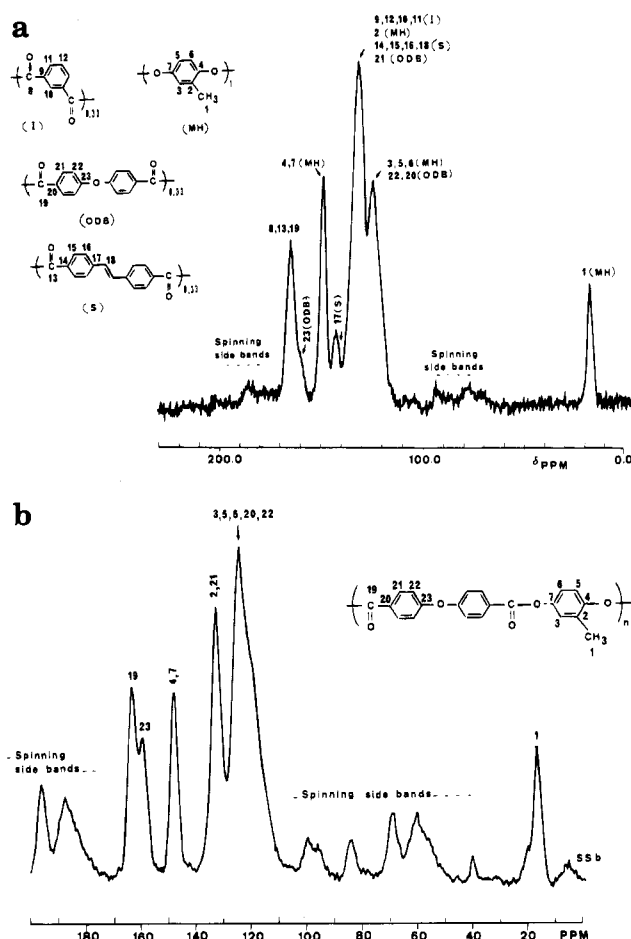t with data obtained for aromatic copolyesters containing methylhydroquinone, isophthaloyl, and/or terephthaloyl units.[23–25]

Copolyesters based on MH, T, S, and ODB were insoluble in virtually all common solvents. However, copolyesters prepared from MH, I, S, and ODB were soluble in p-chlorophenol at high temperatures. The inherent viscosities were between 0.25 and 0.50 dL/g, i.e. significantly lower than the values of 0.52–1.54 and 0.28–1.04 obtained for the intrinsic viscosities of wholly aromatic polyesters prepared from p-acetoxybenzoic acid, hydroquinone diacetate, and I[18] and from ODB, T, and chlorohydroquinone diacetate,[21] respectively.

Thermal Properties and Structure. Homopolyesters. The transition temperatures of homopolyesters are listed in Table 10. The DSC curve of the "as-made" poly(methyl-1,4-phenylene isophthalate) (i.e. the homopolyester MH/I) displayed a marked glass transition between 156 and 164 °C followed by a distinct exotherm (peak at 230 °C) due to cold crystallization; a single melting endotherm appears at 312 °C. The melting enthalpy was about 25 J/g.

The DSC curve of the "as-made" poly(methyl-1,4-phenylene 4,4′-oxydibenzoate) (MH/ODB) exhibited a glass transition between 131 and 143 °C and two endotherms at about 321 and 377 °C. By polarizing microscopy these endothermic peaks were recognized as due to the crystal–nematic (T_m) and nematic–isotropic liquid (T_i) transitions, respectively. These results are in good agreement with the values of 300–340 and 360 °C reported by Kyotani et al.[26] for a polymer with an inherent viscosity of 0.47 dL/g.
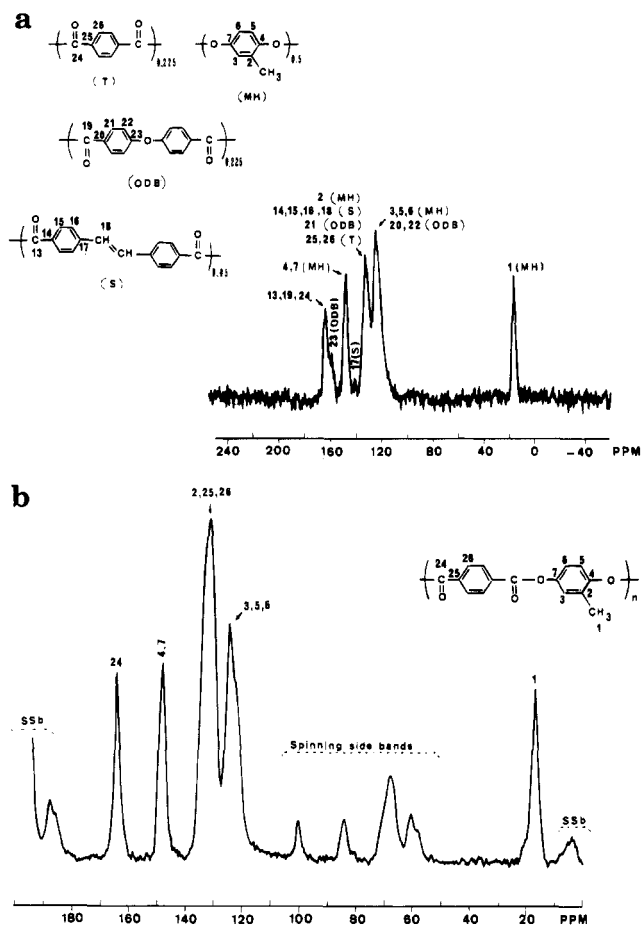
Figure 4. Solid state ^{13}C NMR spectra: (a) copolyester C3; (b) polyester MH/T.

The DSC curve of the "as-made" poly(methyl-1,4-phenylene terephthalate) (MH/T) displayed an endotherm corresponding to the crystal—nematic phase transition that consisted of two overlapping peaks with the main peak at 384 °C. Hot-stage polarizing microscopy revealed that between 360 and 384 °C, this polyester formed a nematic mesophase which persisted up to the thermal stability limit.

The melting temperature of the polyester MH/S is so high (>400 °C) that a stable mesophase is not able to exist without thermal degradation. Thus, replacement of the 1,4-substituted benzene ring (polyester MH/T) by a stilbene group (polyester MH/S) results in a remarkable increase in the melting point consistent with the repeating unit having been elongated.

In contrast with polyesters MH/I and MH/ODB, it was impossible to detect a glass transition in the DSC curves of the fully linear MH/T and MH/S polyesters. It is evident that replacement of angular units such as rigid kinked I units and flexible ODB units by rodlike unsubstituted T or S units causes a substantial increase in the degree of crystallinity. It should be noted that the glass transition temperature of poly(methyl-1,4-phenylene 4,4'-oxydibenzoate) is lower than that of poly-(methyl-1,4-phenylene isophthalate). This supports the expectation that an ether linkage in the repeat unit will give rise to potential flexibility in the chain and hence enable greater conformational freedom.

By comparison of the thermal behaviors of polyesters MH/I and MH/T it appears that the incorporation of rigid kinks such as meta-linked phenyl rings has a drastic influence on the stability of the liquid crystalline phase. It reduces the melting point to 312 °C but also

effectively brings down the clearing point to an even lower temperature and thus prevents liquid crystallinity.

Swivels such as 4,4'-oxydibenzoyl units are also very effective in depressing transition temperatures. The melting point is reduced to 321 °C because of the alterations of chain conformation and diameter that prevent efficient packing in the crystalline state, but the clearing point is less affected so that the polyester MH/ODB exhibits a stable nematic phase.

The effects of introducing lateral substituents into the hydroquinone units are illustrated by reference to polyesters MH/T, MH/ODB, poly(chloro-1,4-phenylene terephthalate),[21,27] and poly(chloro-1,4-phenylene 4,4'-oxydibenzoate),[26,28,29] the methyl group having almost the same size as the chloro group. The use of methyl- or chloro-substituted hydroquinone results in a depression of both the melting point and the clearing temperature of the unsubstituted polymers. The depression may be considered to be partly the result of the steric effects which limit the molecular packing efficiency in both the crystal and the liquid crystal state, but the polar effect is also important and results in a higher clearing temperature for the chloro-substituted polymers.

The principal features of the X-ray powder patterns for polyesters MH/I, MH/T, MH/ODB, and MH/S are given in Table 11.

Coulter et al.[30] have solved the crystalline structure of unsubstituted poly(1,4-phenylene terephthalate) showing that it crystallizes in the monoclinic, $P2_1a$ space group with cell parameters $a = 7.98$ Å, $b = 5.33$ Å, $c = 12.65$ Å, $\alpha = \gamma = 90°$, and $\beta = 98.98°$. Quite recently, Li et al.[31] reported similar results. The diffraction pattern of their powder sample exhibited reflections at 4.86 (w), 4.37 (vs), 3.90 (m), 3.16 (m), 2.97 (m), and 2.69 Å (w) in good agreement with those found by Coulter et al.[30] From Table 11, it is evident that poly(methyl-1,4-phenylene terephthalate) has different interplanar spacings and hence a different crystalline structure, thus showing that methyl substitution does significantly affect the crystal structure of poly(1,4-phenylene terephthalate).

The X-ray powder diffraction pattern of poly(methyl-1,4-phenylene isophthalate) differs from that of poly-(1,4-phenylene isophthalate) reported by Erdemir et al.[18] Some reflections that are found in the powder diffraction pattern of poly(1,4-phenylene isophthalate) are missing. In addition two new reflections appear at 4.67 and 3.68 Å. The X-ray diffraction pattern of polyester MH/I also differs from those of the crystal forms assigned by Blundell et al.[19] and Johnson et al.[32] to the $(I-H)_n$ sequences in aromatic copolyesters containing monomer residues of p-hydroxybenzoic acid, isophthalic acid, and hydroquinone. From Table 11, it is evident that polyester MH/I has different interplanar spacings and hence a different crystalline structure.

The "as-made" polyester MH/ODB is fibrous in form and thus suited to X-ray studies on oriented material. The diffraction pattern shows meridional reflections consistent with a unit cell having a c dimension of 16.7 Å, in good agreement with the length of the MH—ODB repeat unit ($L \approx 16.2$ Å) calculated for the fully extended conformation.

Copolyesters Based on MH, I, and S. "As-Made" Copolyesters. A melting endotherm was observed in the thermograms of the "as-made" low-molecular weight copolyesters A2, A6, A8, and A9. The DSC curve of

Table 10. Effect of Composition on Thermal Properties of "As-Made" and Annealed Homopolymers Based on MH and I, T, ODB, or S

		"as-made" polyester					"annealed" polyester: 300 °C, 15 h		
homopolyester	conversion b (%)	T_g (°C)	T_m (°C)	ΔH (J/g)	T_i (°C)	ΔH (J/g)	T_m (°C)	ΔH (J/g)	weight loss (%)
MH/I	94	156	312[a]	25.3			361	64.7	1.3[b]
MH/T	91	c	360, 384	18.2	c		372, 387	60.3	1.5[b]
MH/ODB	96	131	321	21.3	377	7.5	344	31.9	2.2[b]
MH/S	75	c	c				c		14.2[b]

[a] Cold crystallization occurs in the temperature range 210–243 °C. Exotherm maximum: 230 °C. [b] Determined by TGA. [c] Undetected.

Table 11. Principal Reflections (Å) of Homopolyesters Based on MH and I, T, ODB, or S

MH/I	MH/T	MH/ODB	MH/S
5.98 (vw)	10.36 (w)	16.7[a] (m)	16.14[a] (vw)
5.08 (s)	9.24 (m)	14.46 (w)	8.02[a] (vw)
4.67 (vw)	5.87 (vw)	9.18 (vvw)	6.43 (m)
3.68 (m)	5.47 (w)	5.85 (w)	6.09 (m)
3.52 (m)	4.96 (m)	5.05 (m)	5.31 (vs)
3.37 (w)	4.51 (vs)	4.70 (s)	4.84 (vw)
3.21 (w)	4.25 (w)	4.05 (m)	4.5 (s)
	3.92 (m)	3.46 (vw)	4.19 (w)
	3.75 (m)	3.37 (m)	4.02[a] (w)
	3.43 (w)	3.27 (m)	3.61 (w)
	3.30 (s)		3.45 (s)
	2.98 (w)		3.34 (m)
			3.20[a] (w)
			3.03 (m)

[a] Diffraction peaks which are chain-length-dependent (001) type reflections.
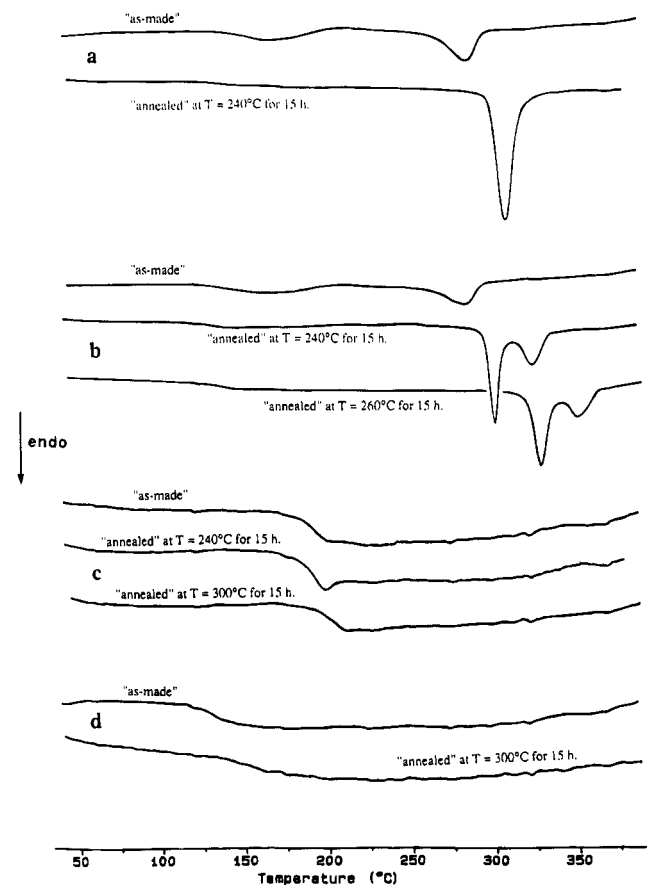
Figure 5. DSC curves of "as-made" and annealed copolyesters A2 (a), A6 (b), A1 (c), and A10 (d).

copolyester A6 featured a broad endotherm, the melting peak overlapping the isotropization peak (Figure 5). Accurate determination of melting and isotropization enthalpies was hindered by difficulties in establishing the baseline position. It should be noted, however, that for the copolyesters A2, A6, A8, and A9 containing stilbene units the total enthalpy change due to melting and isotropization (8–16 J/g) was significantly lower than the value of 25 J/g obtained for the homopolymer based on MH and I (Table 10). This points out that copolymerization of monomer units of different lengths, lateral substitution of aromatic rings, and introduction of rigid kinks to prevent long straight sequences frustrate the formation of crystalline species. In addition, such low enthalpy changes can be rationalized in terms of disorder in the crystalline species, as is evident from the limited diffraction effects.

The DSC curves of all "as-made" copolyesters MH/I/S exhibited a marked glass transition. As expected, the glass transition of the copolyesters of higher molecular weight was shifted to a higher temperature in comparison with that found for the lower molecular weight materials (see Table 12; A2 and A3; A6 and A7; A8, A9, A10).

"As-made" polymer observations using a polarizing microscope indicated that copolymers A1 (i.e. the 85/15 I/S molar ratio) gave a clear isotropic melt. For copolyesters A3, A4, A5, A7, and A10, no fluid mesophase could be detected up to 360 °C. The low molecular weight copolyester A2, A6, A8, and A9 melts showed a strong opalescence between T_m and T_i. Optical observations of copolyesters A2 and A6 did not reveal any particular morphological feature useful in defining the type of mesophase (Figure 6). It is well-known, however, that copolymerization, lateral substitution of aromatic rings and introduction of nonlinear rigid units retain the essential linearity and chain stiffness but inhibit close and regular packing, favoring the formation of nematic mesophases rather than smectic ones. Polarized light micrographs depicting the appearance of copolyesters A8 and A9 exhibit characteristic features of nematic phases, as illustrated in Figures 7 and 8. When the isotropic phase was cooled, the mesophase appeared at the clearing point in the form of typical droplets which, after further cooling, grew and joined together to form larger structures from which stable schlieren textures finally formed. These textures showed an irregular network of black brushes branching out from a number of scattered points or "nuclei", and passing continuously from one nucleus to another. Four brushes met at some nuclei (singularities with $S = \pm 1$) and two at others (singularities with $S = \pm^{1}/_{2}$).

X-ray investigation revealed the semicrystalline character of low molecular weight copolyesters A2, A6, A8, and A9. As shown in Figure 9, the X-ray patterns show a few sharp reflections revealing the presence of ordered crystalline domains and a diffuse halo corresponding to nematic regions frozen in the glassy state. This broad halo corresponds to spacings of about 4.74–4.85 Å. This represents the average interchain distance.

An increase in the conversion (i.e. the molecular weight) brings about a significant change in structure: the degree of order drops. No melting endotherm could

Table 12. Effect of Composition on Thermal Properties of "As-Made" and Annealed Copolyesters Based on MH, I, and S
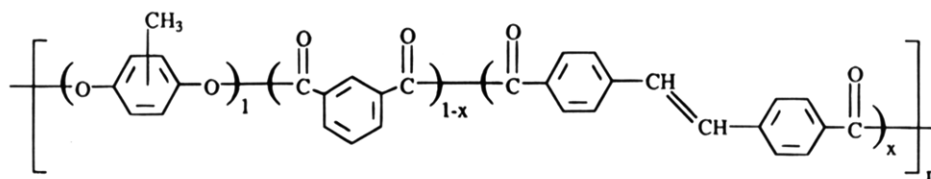
copolyester	composition (mol %) I	composition (mol %) S	conversion b (%)	"as-made" copolyester T_g (°C)	"as-made" copolyester T_m (°C)	"as-made" copolyester T_i (°C)	240 °C (15 h) T_g (°C)	240 °C (15 h) T_m (°C)	240 °C (15 h) T_i (°C)	260 °C (15 h) T_g (°C)	260 °C (15 h) T_m (°C)	260 °C (15 h) T_i (°C)	300 °C (15 h) T_g (°C)	300 °C (15 h) T_m (°C)
MH/I	100	0	94	156	312[c]					168.6	318			361
A1	85	15	92	180	320–330[b]		182.7			181.8			193.5	
A2	80	20	84	140	283	315–320[b]	168	305					182.8	
A3	80	20	97	173			177			176.7			182.8	
A4	75	25	91	173			180			183.6			203.8	
A5	70	30	89	178			178			188			205.4	
A6	65	35	86	125	281[a]		127	300	323	128	325	347		
A7	65	35	95	132			130, 155			127, 160			133, 180	
A8	50	50	47	95	276	343	101.3	283	344	106	292	345		
A9	50	50	72.5	95	276	363.8	101	280	364					
A10	50	50	94	124.5									143.7	

[a] Broad peak, the melting endotherm overlaps the isotropization endotherm. [b] Assessed by hot-stage microscopy. [c] Cold crystallization occurs in the temperature range 210–243 °C. Exotherm maximum: 230 °C.
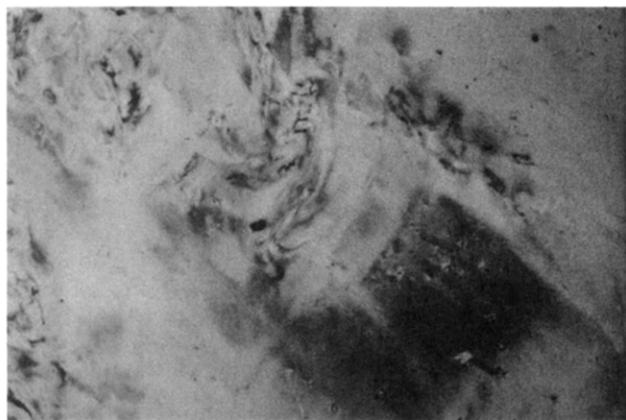
Figure 6. Ill-defined texture of the copolyester A2 at $T = 299$ °C. Crossed polarizers.
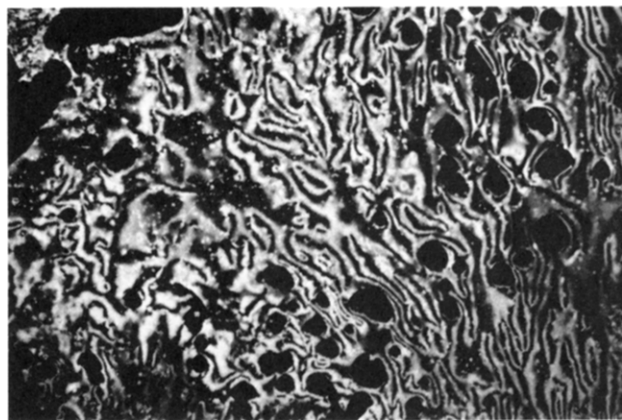
Figure 8. Texture of the nematic phase of copolyester A9 at $T = 295$ °C. Crossed polarizers.
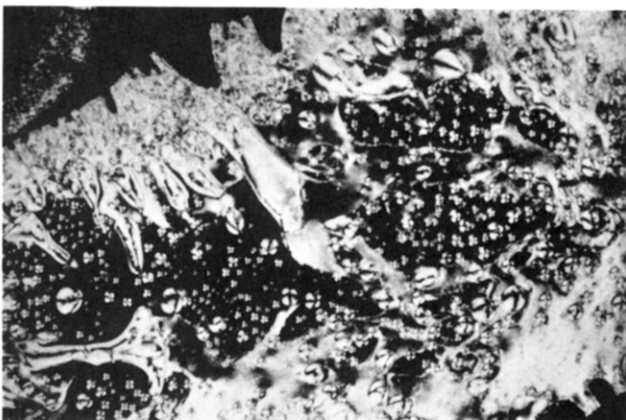
Figure 7. Texture of the nematic phase of copolyester A8 at $T = 311$ °C. Crossed polarizers.
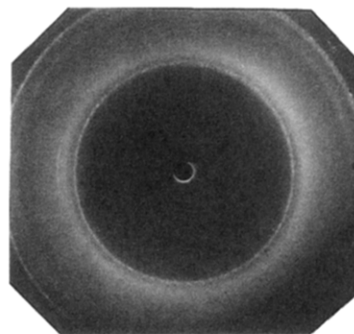
Figure 9. X-ray diffraction pattern of "as-made" copolyester A8. Powder sample at room temperature.

be detected due to the very low level of crystallinity present. Hot-stage optical microscopy indicated that the copolyesters A3, A4, A5, A7, and A10 began to soften at about 280–300 °C. The X-ray patterns of these copolyesters are characterized by a broad diffuse halo, indicating a lack of periodic lateral order and corre-

sponding to an average interchain distance of 4.75–4.85 Å.

To summarize, in the composition range I/S from 80/20 to 50/50, the "as-made" copolyesters form a nematic phase in agreement with the stir opalescence observed during the polymerization. The degree of order and the transition temperatures strongly depend on the monomer conversion at the end of polymerization. For example, the copolyester A2 (i.e. the 80/20 I/S molar ratio, b = 84%) exhibits a glass transition at 140 °C, a
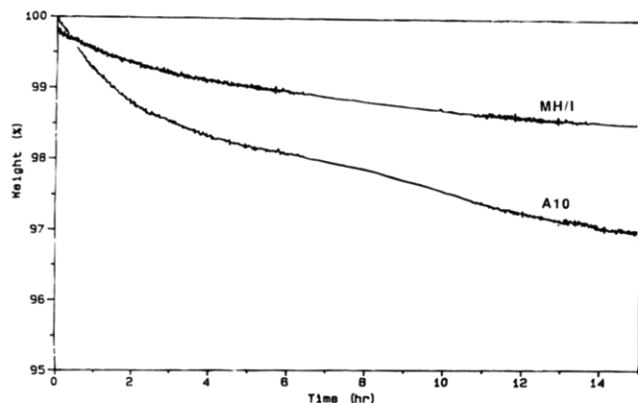
Figure 10. Thermogravimetric analysis of polymers MH/I and A10 in N_2 at 300 °C.

melting endotherm at 283 °C, and a clearing peak at 315–320 °C whereas the higher molecular weight copolyester A3 (i.e. the same I/S molar ratio, but b = 97%) displays only a glass transition at 173 °C. Hence, we can compare only the "as-made" polymers obtained with roughly equivalent monomer conversions (i.e. MH/I, A1, A3, A4, A5, A7, and A10). As expected, the inclusion of extented rigid S units first increases T_g and T_m. Quite surprisingly, however, the glass transition temperature decreases, as the S content in the diacid mixture used for the copolycondensation is 35 mol % high or higher.

Annealed Copolyesters. The results of different thermal treatments show that all the copolyesters were substantially affected by annealing in terms of both transition temperatures and enthalpy changes (Figure 5). TGA measurements showed that less than 1% weight loss occurred upon annealing at 240 or 260 °C for 15 h. However, after annealing at 300 °C for 15 h weight losses ranged from 1.3 to 3.3% (Figure 10), probably due to postpolycondensation. It should be noted, however, that stilbene is thermally less stable than other components. The double bond may undergo decomposition and cross-linking reactions above ~260 °C. This point will be discussed later.

Annealing of the "as-made" polymers MH/I, A2, A6, A8, and A9 at 240 °C for 15 h resulted in an increase in the melting temperature (Table 12). The melting endotherm also became stronger and slightly sharper (Figure 5). After thermal treatment, the melting enthalpy of homopolyester MH/I (ΔH = 44.5 J/g) was significantly higher than the value of 25 J/g obtained for the "as-made" material (Figure 11). For the copolyesters, the total enthalpy changes due to melting and isotropization increased from 10–15 to 20–30 J/g. As expected, an increase in the annealing temperature results in an increase in both the melting temperature and the enthalpy change. Thus, annealing homopolyester MH/I at 300 °C for 15 h resulted in a melting peak at 361 °C and a melting enthalpy of 64.7 J/g.

The powder X-ray diffraction patterns of copolyesters A2, A6, and A8 also revealed the development of crystalline order on annealing. Compared with the "as-made" copolyesters, the diffuse halo is less intense and there are reflections which are stronger and/or sharper (Figure 12). Copolymerization results in a disruption of the crystal structure of poly(methyl-1,4-phenylene isophthalate) (Tables 11 and 13). The para-linked S units cannot be accommodated easily in the "MH/I" unit cell. The X-ray diffraction patterns of the copolyesters A2 and A6 (where the I/S ratio is 80/20 and 65/35,
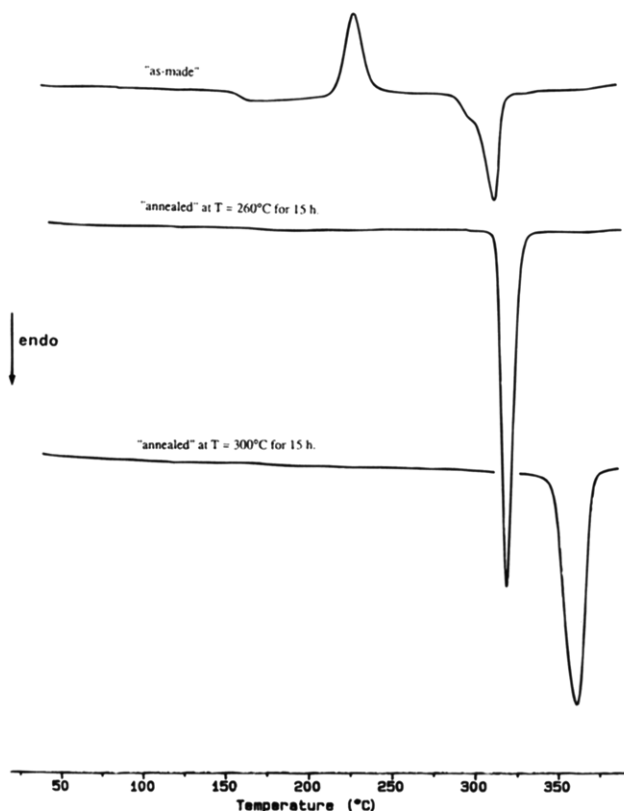

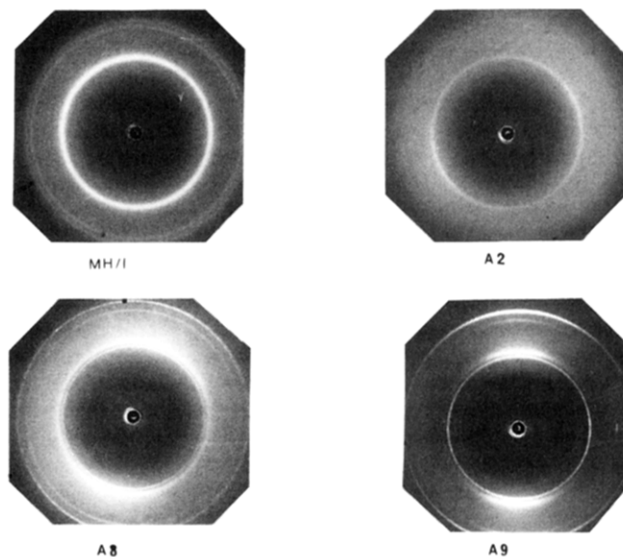**Figure 11.** DSC curves of "as-made" and annealed copolyester MH/I.

Figure 12. X-ray diffraction patterns of polyester MH/I and copolyesters A2, A8, and A9 after annealing at 240 °C for 10 h.

respectively) show only three rings with d spacings of about 5.00–5.03, 3.65, and 3.48–3.49 Å. This indicates the same lateral chain packing as in the "MH/I" modification. With a further increase in the concentration of elongated and fairly rigid S units, the 5.00–5.03 reflection decreases in intensity. In the X-ray diffraction pattern of fibrous copolyester A9 this reflection is present only as two weak arcs along the equator (Figure 12). However, there are new reflections at 15.7–15.86, 6.13, 5.28, 3.96–3.99, and 3.39–3.40 Å which are also found in the powder diagram of polyester MH/S (Table 11). This indicates the existence of another type of structure, which is rather similar to the MH/S modification. This kind of behavior was observed by Erdemir

Table 13. Principal Reflections (Å) of Copolyesters Based on MH, I, and S after Annealing at 240 °C for 10 h

A2	A6	A8	A9
		15.86 (vw)	15.7 (vw) [15.72[a]]
5.00 (s)	5.03 (s)	5.28 (m)	6.13 (m) [6.10[a]]
		5.01 (s)	5.87 (w)
		3.99 (vw)	5.28 (s)
3.65 (m)	3.65 (m)	3.64 (m)	4.98 (vw)
3.48 (m)	3.49 (m)	3.50 (w)	3.96 (vw)
		3.39 (m)	3.63 (m)
			3.40 (m)

[a] Observed with oriented fibers.

et al.[18] for wholly aromatic copolyesters prepared from p-acetoxybenzoic acid, hydroquinone diacetate, and isophthalic acid. The 75/25 copolymer has a poorly ordered pseudohexagonal structure which is similar to the lateral chain packing of poly(p-oxybenzoate) in the high-temperature modification. This structure, termed modified A, persists in the 67/33 and 50/50 copolymers. However, these two copolymers also contain a type of structure, termed modified B, which is rather similar to that of poly(p-phenylene isophthalate).

Annealing of higher molecular weight copolyesters A1, A3, A4, A5, A7, and A10 resulted in an increase in the glass transition temperature. No melting endotherm could be detected, suggesting that crystallization was hindered by the high viscosity of the melts. Further evidence for this lack of crystallinity was obtained from X-ray diffraction studies of stretched oriented fibers. The X-ray patterns obtained using fibers were qualitatively like those for oriented samples of low molar mass nematic phases. They were characterized by two symmetrical wide-angle diffuse crescents, indicating a lack of periodic lateral order and corresponding to an average interchain distance of 4.7–4.8 Å. A high degree of orientation could be obtained, but even these highly oriented samples did not exhibit a noticeable degree of crystallinity. Recently, Sinta et al.[33] reported that completely aromatic, para-linked, 2,2'-substituted biphenyl and substituted phenyl polyesters did not show any tendency to crystallize even after days of annealing. They postulated that the combination of lateral substituents, comonomers of different lengths, and the enantiomeric, noncoplanar biphenyls completely eliminates crystallinity by diminishing interchain interactions. Annealing carried out at 240 and 260 °C only

slightly affected the glass transition temperature (Table 12). However, an increase in the annealing temperature to 300 °C resulted in a significant shift of the glass transition temperature. This effect was found to be dependent on the conversion of monomer to polymer at the end of polymerization (hence molecular weight). The most substantial increase in the glass transition temperature was found for copolyesters A4 (b = 91%) and A5 (b = 89%) corresponding to the lower conversions while the smallest one was observed for copolyester A3 (b = 97%). These observations, coupled with the TGA data presented previously, indicate that postpolycondensation reactions occur at 300 °C, resulting in an increase in the molecular weight of the samples.

Copolyesters Based on MH, I, S, and ODB. "As-Made" Copolyesters. The transition temperatures obtained from DSC thermograms, and confirmed by hot-stage light microscopy, are given in Table 14.

There was no real evidence for liquid crystal properties in the "as-made" copolyesters B1, B3, B4, B7, B8, and B9. Rather, these copolyesters resembled typical amorphous polymers. Copolyesters B1, B3, B4, and B7 started to flow at about 210, 320, 300–310, and 290–300 °C, respectively. No fluidity could be detected below and at 360 °C for copolyesters B8 and B9. This probably results from the high S content.

The DSC traces of the "as-made" copolyesters B2, B5, and B6 were characterized by a glass transition and one or two endotherms corresponding to a crystal–liquid crystal transition followed by a liquid crystal–isotropic transition (Figure 13). The melting enthalpies were between 2 J/g (copolyesters B5 and B6) and 5 J/g (copolyester B2), i.e. significantly lower than the values found for the copolyesters A2, A6, A8, and A9. This can be considered to be the outcome of a deliberate design feature whereby three diacids of different lengths were used to disrupt the regularity of the chain in order to frustrate the formation of stable crystals. No typical texture could be obtained even after annealing for hours. However, the X-ray diffraction patterns obtained using oriented fibers were consistent with the existence of nematic phases. They consisted of two symmetrical wide-angle diffuse crescents related to the average intermolecular spacing (Figure 14).

From the results summarized in Table 14, the following points can be established:

Table 14. Effect of Composition on Thermal Properties of "As-Made" and Annealed Copolyesters Based on MH, I, S, and ODB

| copolyester	composition (mol %)			conversion b (%)	η_{inh} (dL/g)	"as-made" copolyester			annealed copolyester			
									230 °C (15 h)		280 °C (15 h)	300 °C (15 h)
	I	S	ODB			T_g (°C)	T_m (°C)	T_i (°C)	T_g (°C)	T_m (°C)	T_g (°C)	T_g (°C)
B1	50	0	50	97	0.53	151					178	172.6
B2	76	19	5	84	0.25	149	269	320[a]	153	293		
B3	72	18	10	90	0.33	162			162.3		171	
B4	64	16	20	87	0.32	146.4			153		170	
B5	60	20	20	87	0.31	120	249	330–340[a]	120	288		
B6	50	20	30	86	0.30	116	235[a]	360[a]	119	285		
B7	45	10	45	85	0.28	154			150		165	
B8	33.3	33.3	33.3	82	0.32	118.5					124	135
B9	20	40	40	95	0.50	118						

[a] Assessed by hot-stage microscopy.
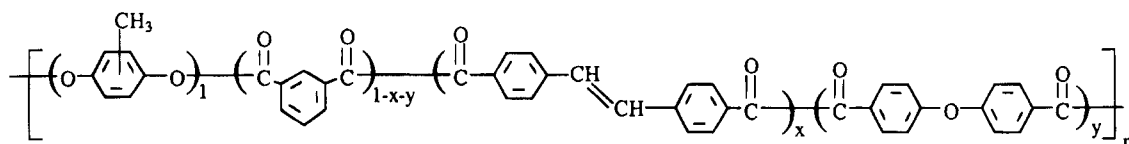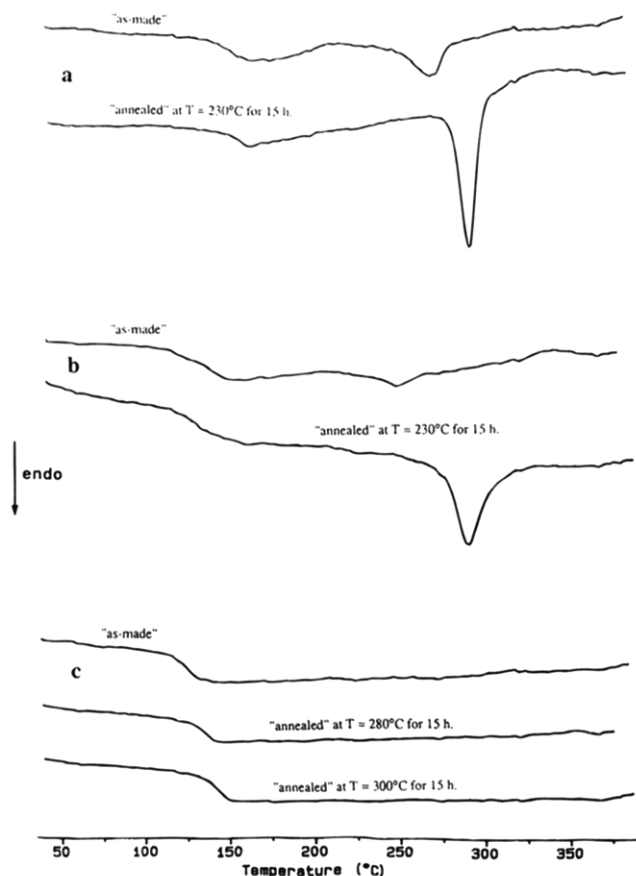
Figure 13. DSC curves of "as-made" and annealed copolyesters B2 (a), B5 (b), and B8 (c).
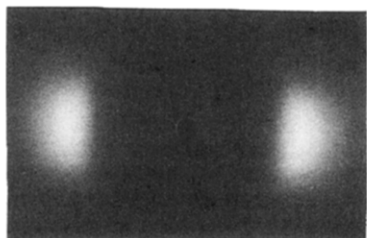

Figure 14. X-ray diffraction pattern of the oriented nematic phase taken from a stretching-oriented fiber of copolyester B5.

(i) An S content of at least 20% in the I/S/ODB mixtures is required for liquid crystal formation.

(ii) Replacement of I by ODB in the diacid mixtures containing about 20% S (A2, B2, B5, and B6) results in a decrease of the melting temperature and enthalpy change, but an increase in the isotropization temperature. Hence, the temperature range of the mesophase is much larger for B6 (I/S/ODB: 50/20/30, $\Delta T \approx 125$ °C) than for A2 (I/S/ODB: 80/20/0, $\Delta T \approx 35$ °C). However, the glass transition is shifted to a lower temperature: ODB can give rise to potential flexibility in the chain.

(iii) As observed for the MH/I/S system, high S content (≥ 33.3 mol %) in the diacid mixture used for the copolycondensation yields copolyesters with relatively low glass transition temperatures.

Annealed Copolyesters. As expected, annealing of the "as-made" copolyesters B2, B5, and B6 at 230 °C for 15 h resulted in an increase in the melting temperature and enthalpy change, but there was no significant shift of the glass transition (Figure 13). It should be noted that the melting enthalpies remained substantially low ($11-14$ J/g) in comparison with those found for the MH/I/S copolyesters. The increase in the degree
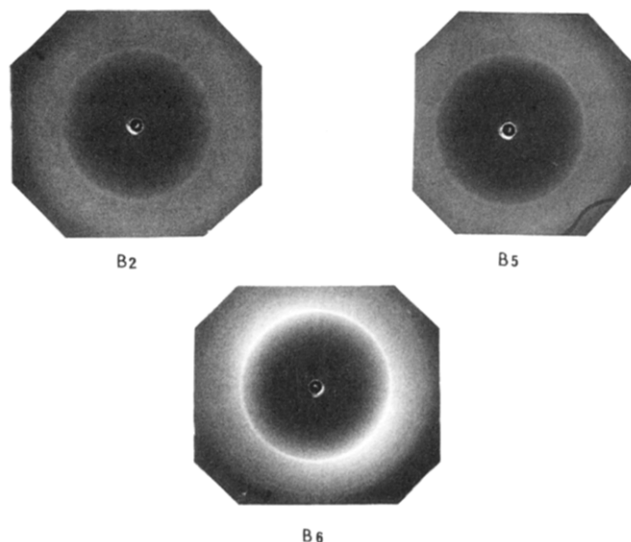

Figure 15. X-ray diffraction patterns of copolyesters B2, B5, and B6 after annealing at 210 °C for 10 h.

Table 15. Principal Reflections (Å) of Copolyesters Based on MH, I, S, and ODB after Annealing at 210 °C for 10 h

| B2	B5	B6
	15.59 (vw)	15.41 (vw)
5.03 (vs)	4.97 (vs)	5.02 (vs)
		4.71 (vw)
3.64 (m)	3.62 (m)	3.63 (m)
3.46 (w)	3.46 (w)	3.46 (m)

of crystallinity with annealing can be further supported by X-ray diffraction studies. As shown in Figure 15, the powder X-ray diffraction patterns exhibit a few well-defined rings corresponding to the lattice spacings given in Table 15. The X-ray diffraction patterns of the copolyesters A2 (I/S/ODB: 80/20/0 mol %) and B2 (I/S/ODB: 76/19/5 mol %) show that a slight modification of the diacid mixture composition does not have any appreciable effect on the structure. The X-ray pattern of copolyester B2 exhibits only those reflections found in the copolyester A2 and assigned to the type "MH/I" structure. A further increase in the ODB/I ratio results in the appearance of two new reflections at spacings of $15.4-15.6$ and 4.71 Å, which are also found in the MH/ODB homopolyester pattern. This indicates the existence of another type of structure similar to the MH/ODB modification. Hence, the ordered structure is again highly dependent upon composition.

Again, the annealing carried out at 230 °C did not have any appreciable effect on the glass transition temperature of the amorphous copolyesters. However, an increase in the annealing temperature to 280 °C resulted in a significant shift of the glass transition to higher temperature, probably due to an increase in the molecular weight resulting from postpolycondensation reactions. TGA experiments revealed reduced stability of copolyesters B at 300 °C. At this temperature most of the copolyesters B exhibit appreciable weight loss, which cannot be explained only in terms of post polycondensation reactions. For example, 14.8% weight loss occurred upon annealing copolyester B1 at 300 °C for 15 h. Evidence for degradation is obtained from the glass transition temperature of 172.6 °C, slightly lower than that obtained upon annealing copolyester B1 under the same conditions, but at 280 °C.

Copolyesters Based on MH, T, S, and ODB. The transition temperatures obtained from DSC traces and

Table 16. Effect of Composition on Thermal Properties of "As-Made" and Annealed Copolyesters Based on MH, T, S, and ODB

copolyester	composition (mol %)			conversion b (%)	T_g (°C)	"as-made" copolyester				annealed copolyester 240 °C (15 h)		
	T	S	ODB			T_m (°C)	ΔH (J/g)	T_i (°C)		T_g (°C)	T_m (°C)	ΔH (J/g)
C1	50	0	50	98	115.7	264	7.9	>360[a]		113	275	13.2
C2	47.5	5	47.5	90	104.6	272	8.7	>380[a]		105.7	291	13.0
C3	45	10	45	85	115					116		

[a] Assessed by hot-stage microscopy.
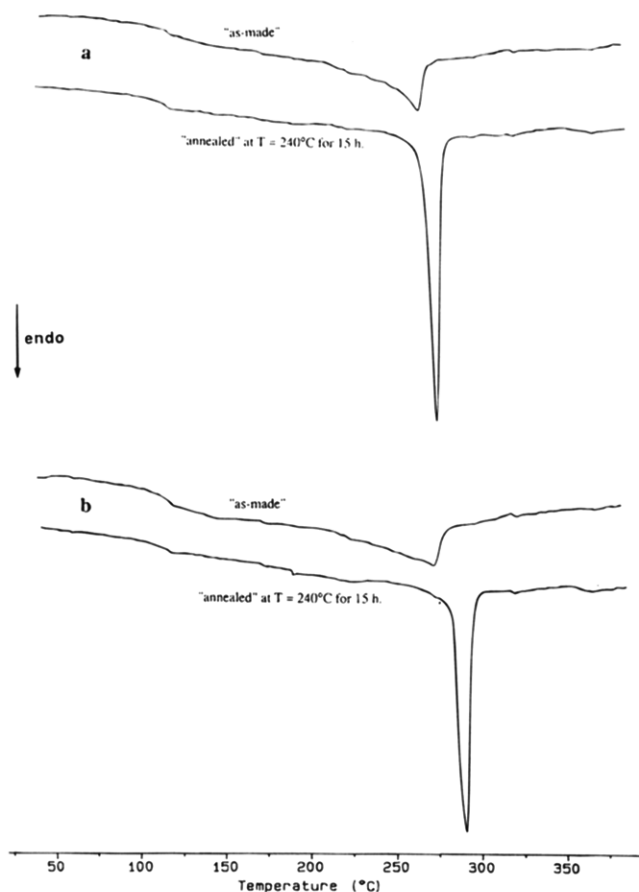
Figure 16. DSC curves of "as-made" and annealed copolyesters C1 (a) and C2 (b).

Figure 17. Texture of the nematic phase of copolyester C2 at $T = 380$ °C. Crossed polarizers.

confirmed by hot-stage light microscopy are given in Table 16.

The DSC curves of "as-made" copolyesters C1 and C2 exhibited a well-defined glass transition and a rather broad melting endotherm (Figure 16). The melting enthalpies were 7.9 and 8.7 J/g, respectively. A small amount of polymer placed between the glass slide and cover slip spontaneously gave rise to an anisotropic fluid that exhibited a typical nematic threaded texture (Figure 17). No clearing point was observed, at least up to 380 °C. Hence, the nematic temperature range of these copolyesters is greater than 100 °C. For copolyester C3 no melting endotherm could be detected due to the low level of crystallinity present. Hot-stage microscopy indicated that this copolymer began to soften at about 315–320 °C. The X-ray diffraction patterns revealed the semicrystalline character of these copolyesters (Figure 18a–c). They showed sharp reflections,

indicating the presence of ordered structure and a diffuse halo or two diffuse crescents related to the average intermolecular spacing characteristic of the chains located in the nematic regions frozen in the glassy state.

As expected, the copolyesters underwent further crystallization on annealing: the melting point and enthalpy change increase (Table 16). Further evidence for this increase in the degree of crystallinity with annealing is obtained from X-ray diffraction studies. Thermal treatment was accompanied by disappearance of the diffuse ring or crescents (Figure 18d,e). However, comparison of the X-ray patterns obtained for "as-made" and annealed copolyesters C immediately leads to the conclusion that annealing did not cause any change in crystal structure. Table 17 lists the main reflections for each C copolyester. The X-ray diffraction pattern of copolyester C1 shows a few reflections that are also found in a powder pattern of homopolyester MH/T, namely the strong reflections at spacings of 4.54 and 4.82 Å. However, some of the reflections characteristic of the type MH/T structure are missing and none of the reflections arising from the type MH/ODB structure can be detected. This indicates the existence of a type of structure rather similar to the type MH/T structure. An increase in the concentration of elongated and fairly rigid S units from 0 to 10 mol % in the diacid mixture does not have any appreciable effect on the X-ray diffraction patterns.

Comparison of data obtained for copolyesters B1 (I/S/ODB: 50/0/50) and C1 (T/S/ODB: 50/0/50) shows that the replacement of the rigid kinked I units by the linear T units results in the appearance of a nematic mesophase. This is in agreement with the requirement
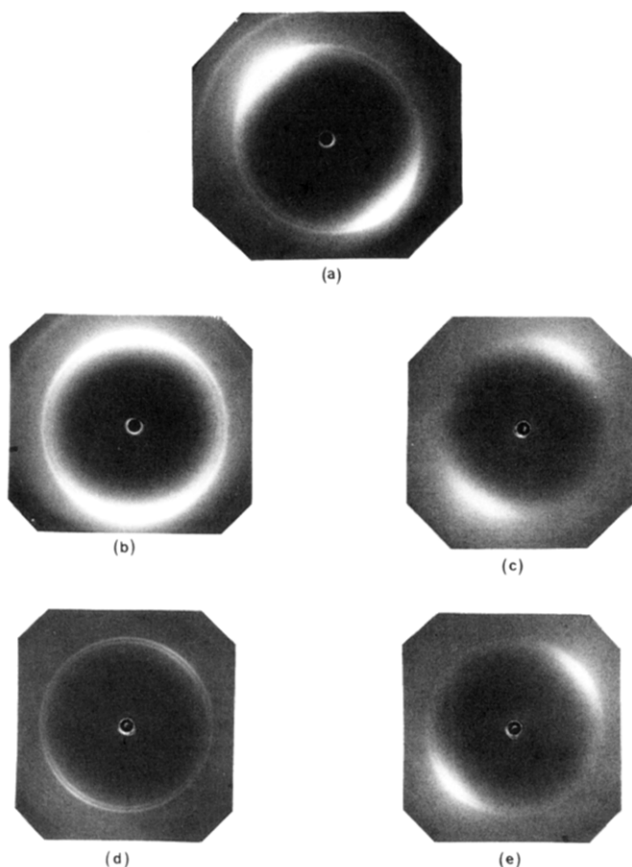
Figure 18. X-ray diffraction patterns of copolyesters C at room temperature: (a)–(c): "as-made" copolyesters C1, C2, and C3; (d) copolyester C2 annealed at 240 °C for 10 h; (e) copolyester C3 annealed at 160 °C for 10 h.

Table 17. Principal Reflections (Å) of Copolyesters Based on MH, T, S, and ODB

C1	C2	C3
9.2 (m)[a]		
5.96 (vw)[a]		5.92 (vw)[a]
4.82 (s)	4.79 (s)	4.82 (m)
4.54 (vs)	4.53 (vs)	4.50 (m)
4.00 (w)		
3.34 (m)	3.36 (m)	3.82 (w)

[a] Observed with oriented fibers.

for forming a mesophase in which the chains contain sufficient rigid linear units to give a chain configuration of high persistence length and aspect ratio.[34] Replacing the isophthalic acid by terephthalic acid also imparts crystallinity, but significantly lowers the glass transition temperature (151 to 116 °C). Similar conclusions can be drawn from the comparison of the thermal behaviors of copolyesters B7 (I/S/ODB: 45/10/45) and C3 (T/S/ODB: 45/10/45).

Conclusion

A number of wholly aromatic copolyesters were prepared from methyl hydroquinone diacetate (MH) and at least two of the following diacids: isophthalic acid (I), stilbenedicarboxylic acid (S), 4,4′-oxydibenzoic acid (ODB), and terephthalic acid (T). The first parent homopolymer of the copolyesters A (MH/I/S) investigated, poly(methyl-1,4-phenylene isophthalate) (MH/I), is a typical isotropic polymer. The rigid angular isophthaloyl units and the methyl-substituted *p*-phenylenedioxy units hinder the formation of the liquid crystalline phase. However, a reaction mixture with I/S ≤ 80/20

mol % results in nematic copolyesters. This points out the importance of the rigid nature of the geometry of stilbene in stabilizing liquid crystals, as illustrated by reference to model compounds in the first paper of this series.[1]

For comparison it is useful to cite earlier papers concerned with the effects of rodlike *p*-oxybenzoyl, *p*-phenylenedioxy, and terephthaloyl units, rigid angular isophthaloyl and *m*-oxybenzoyl disruptors, and methyl-substituted *p*-phenylenedioxy units.[18,21,26–29,35] The unsubstituted fully aromatic poly(1,4-phenylene isophthalate) (H/I) has no mesophase. The angular I units lead to hindered mesophase packing.[18] However, Erdemir et al.[18] have shown that introduction of rodlike *p*-oxybenzoyl units results in poly(*p*-oxybenzoate-*co*-*p*-phenylene isophthalate)s which are nematic in the composition range extending from 50/50 to 75/25. The "as-made" 33/67 and 43/57 copolymers exhibit only a crystal–isotropic liquid transition. However, heating to 460 °C followed by quenching results in a decrease of the melting temperature and the formation of a nematic phase in a narrow temperature range. Blundell et al.[19] have observed the borderline between isotropic and liquid crystal behavior for 20/80 and 27.5/72.5 copolymers in close agreement with the observations of Erdemir et al.[18]

Jackson[36] has investigated the thermal properties of poly(*m*-oxybenzoate-*co*-2-methyl-1,4-phenylene terephthalate). There is evidence that the parent homopolymer of this copolymer series, poly(2-methyl-1,4-phenylene terephthalate) forms a nematic phase. Introduction of angular *m*-oxybenzoyl units prevents long straight sequences. As a result, the "as-made" 50/50 copolymer gives a clear isotropic melt.

Both I and ODB can be used to offset the linearity and perfect regularity of simple but intractable para-linked polyesters. However, some differences exist, as illustrated by reference to copolyesters A (MH/I/S) and copolyesters B (MH/I/ODB/S) investigated here. Replacement of I by ODB in the diacid mixtures containing about 20% S results in a decrease of the melting temperature but an increase in the clearing point. Hence, the temperature range of the mesophase is much larger for copolyesters B than for copolyesters A. It should be noted that the parent homopolymer of the copolyesters A, poly(2-methyl-1,4-phenylene isophthalate) is a conventional polymer with isotropic melt. In contrast, poly(2-methyl-1,4-phenylene 4,4′-oxydibenzoate) is a thermotropic nematic polymer. This points out the importance of the rigid nature of the angular isophthaloyl units in destabilizing liquid crystals. Flexible angular 4,4′-oxydibenzoyl units are less efficient. There is prior evidence for this. Poly(chloro-1,4-phenylene terephthalate) is a thermotropic nematic polymer.[27,35] Introduction of 4,4′-oxydibenzoyl units results in poly(chloro-1,4-phenylene terephthalate-*co*-4,4′-oxydibenzoate)s which are nematic throughout the whole composition range.[21] Poly(chloro-1,4-phenylene-4,4′-oxydibenzoate) has also been reported to be nematic.[26,28,29]

Comparison of data obtained for the copolyesters B1 (MH/I/ODB/S: 100/50/50/0) and C1 (MH/T/ODB/S: 100/50/50/0) shows that the replacement of the rigid angular isophthaloyl units by the rodlike terephthaloyl units results in the appearance of a nematic phase. As expected, copolyester C1 has sufficiently rigid chains for the formation of a mesophase. An S content of at least 20% in the I/ODB/S mixtures is required for obtaining thermotropic copolyesters B.

Interpretation of the X-ray diffraction patterns obtained for the semicrystalline copolyesters led to the conclusion that the ordered structure is strongly dependent upon heat treatment and copolymer composition. As expected, copolyesters underwent further crystallization on annealing. There were an enhancement of the order and an increase of the melting temperature and enthalpy change. However, thermal treatment carried out below the melting point of the "as-made" copolyesters did not cause any change in ordered structure. For each copolyester series two distinct crystalline forms are observed. They are similar to the ordered structures of the parent homopolymers. In the middle composition range both types of structure may coexist.

References and Notes

(1) Leblanc, J. P.; Tessier, M.; Judas, D.; Friedrich, C.; Noël, C.; Maréchal, E. *Macromolecules* **1993**, *26*, 4392.
(2) Noël, C.; Navard, P. *Prog. Polym. Sci.* **1991**, *16*, 55.
(3) Cao, M.-Y.; Wunderlich, B. *J. Polym. Sci., Polym. Phys. Ed.* **1985**, *23*, 521.
(4) Butzbach, G. D.; Wendorff, J. H.; Zimmermann, H. J. *Makromol. Chem., Rapid Commun.* **1985**, *6*, 821.
(5) Butzbach, G. D.; Wendorff, J. H.; Zimmermann, H. J. *Polymer* **1986**, *27*, 1337.
(6) Sauer, T. H.; Zimmermann, H. J.; Wendorff, J. H. *Colloid Polym. Sci.* **1987**, *265*, 210.
(7) Bechtoldt, H.; Wendorff, J. H.; Zimmermann, H. J. *Makromol. Chem.* **1987**, *188*, 651.
(8) Sauer, T. H.; Wendorff, J. H.; Zimmermann, H. J. *J. Polym. Sci., Polym. Phys. Ed.* **1987**, *25*, 2471.
(9) Cheng, S. Z. D. *Macromolecules* **1988**, *21*, 2475.
(10) Cheng, S. Z. D.; Janimak, J. J.; Zhang, A.; Zhou, Z. *Macromolecules* **1989**, *22*, 4240.
(11) Kaito, A.; Kyotani, M.; Nakayama, K. *Macromolecules* **1990**, *23*, 1035.
(12) Wilson, D. J.; Vonk, C. G.; Windle, A. H. *Polymer* **1993**, *34*, 227.
(13) Blackwell, J.; Cheng, H.-M.; Biswas, A. *Macromolecules* **1988**, *21*, 39.
(14) Stamatoff, J. B. *Mol. Cryst. Liq. Cryst.* **1984**, *110*, 75.
(15) Blundell, D. J. *Polymer* **1982**, *23*, 359.
(16) Wunderlich, B. *Crystal Melting*; Macromolecular Physics; Academic: New York, 1980; Vol. 3.
(17) Wunderlich, B.; Grebowicz, J. *Fortschr. Hochpolym. Forsch.* **1984**, *60/61*, 1.
(18) Erdemir, A. B.; Johnson, D. J.; Tomka, J. G. *Polymer* **1986**, *27*, 441.
(19) Blundell, D. J.; Mac Donald, W. A.; Chivers, R. A. *High Perform. Polym.* **1989**, *1*, 97.
(20) Toland, W. G.; Wilkes, J. B.; Brutschy, F. J. *J. Am. Chem. Soc.* **1953**, *75*, 2263.
(21) McIntyre, J. E.; Maj, P. E. P.; Sills, S. A.; Tomka, J. G. *Polymer* **1987**, *28*, 1971.
(22) O'Mahoney, C. A.; Williams, D. J.; Colquhoun, H. M.; Blundell, D. J. *Polymer* **1990**, *31*, 1603.
(23) Leblanc, J. P.; Tessier, M.; Maréchal, E. To be published.
(24) Gérard, A. Thèse de Doctorat de l'Université Pierre et Marie Curie, Paris, 18 Décembre 1991.
(25) Noël, C.; Friedrich, C.; Lauprêtre, F.; Billard, J.; Bosio, L.; Strazielle, C. *Polymer* **1984**, *25*, 263.
(26) Kyotani, M.; Yoshida, K.; Ogawara, K.; Kanetsuna, H. *J. Polym. Sci. Part B: Polym. Phys.* **1987**, *25*, 501.
(27) Krigbaum, W. R.; Hakemi, H.; Kotek, R. *Macromolecules* **1985**, *18*, 965.
(28) Du Pont (Schaefgen, J. R.; et al.) Br. Pat. 1 507 207 (priority to May 1974, U.S.A.).
(29) Du Pont (Kleinschuster, J. J.) U.S. Pat. 3 991 014 (priority 16 July 1975).
(30) Coulter, P. D.; Hanna, S.; Windle, A. H. *Liq. Cryst.* **1989**, *5*, 1603.
(31) Li, Z. G.; McIntyre, J. E.; Tomka, J. G.; Voice, A. M. *Polymer* **1993**, *34*, 1946.
(32) Johnson, D. J.; Karacan, I.; Tomka, J. G. *Polymer* **1993**, *34*, 1749.
(33) Sinta, R.; Gaudiana, R. A.; Minus, R. A.; Rogers, H. G. *Macromolecules* **1987**, *20*, 2374.
(34) Flory, P. J. *Proc. R. Soc.* **1956**, *A234*, 60.
(35) Lenz, R. W.; Jin, J. I. *Macromolecules* **1981**, *14*, 1405.
(36) Jackson, W. J. *Br. Polym. J.* **1980**, *12*, 154.